LANGMUIR Article
Cite This: Langmuir 2018, 34, 11076−11085
pubs.acs.org/Langmuir

Controlling Foam Stability with the Ratio of Myristic Acid to Choline Hydroxide

Audrey Arnould,[†] Fabrice Cousin,[‡] Anniina Salonen,[§] Arnaud Saint-Jalmes,[∥] Adrian Perez,[⊥] and Anne-Laure Fameau*[,†]

[†]Biopolymères Interactions Assemblages INRA, la Géraudière, 44316 Nantes, France
[‡]Laboratoire Léon-Brillouin, CEA Saclay, 91191 Gif-sur-Yvette CEDEX, France
[§]Laboratoire de Physique des Solides, UMR 8502, Université of Paris Sud, 91405 Orsay, France
[∥]Institut de Physique de Rennes, UMR CNRS 6251-Université Rennes 1, Rennes 35042, France
[⊥]Grupo de Biocoloides, Instituto de Tecnología de Alimentos, Universidad Nacional del Litoral, 1 de Mayo 3250, Santa Fe 3000, Argentina

Supporting Information

ABSTRACT: The interfacial and foam properties of a model system based on the mixture between myristic acid and choline hydroxide have been investigated as a function of the molar ratio (R) between these two components and temperature. The aim of this study was to obtain insight on the links between the self-assemblies in bulk and in the foam liquid channels, the surfactant packing at the interface, and the resulting foam properties and stability. A multiscale approach was used combining small angle neutron scattering, specular neutron reflectivity, surface tension measurements, and photography. We highlighted three regimes of foam stability in this system by modifying R: high foam stability for $R < 1$, intermediate at $R \sim 1$, and low for $R > 1$. The different regimes come from the pH variations in bulk linked to R. The pH plays a crucial role at the molecular scale by setting the ionization state of the myristic acid molecules adsorbed at the gas−liquid interface, which in turn controls both the properties of the monolayer and the stability of the films separating the bubbles. The main requirement to obtain stable foams is to set the pH close to the pK_a in order to have a mixture of protonated and ionized molecules giving rise to intermolecular hydrogen bonds. As a result, a dense monolayer is formed at the interface with a low surface tension. R also modifies the structure of self-assembly in bulk and therefore within the foam, but such a morphological change has only a minor effect on the foam stability. This study confirms that foam stability in surfactant systems having a carboxylic acid as polar headgroup is mainly linked to the ionization state of the molecules at the interface.

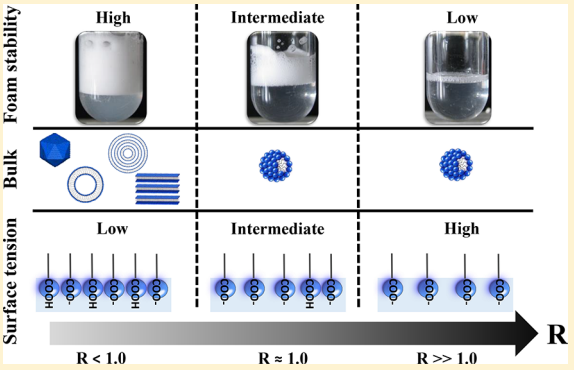

INTRODUCTION

Fatty acid soaps have been known for over 2000 years as surfactants to produce foams and emulsions, and have been used for a long time in laundry and personal care products.[1−4] Fatty acids are anionic surfactants with a carboxylic acid as polar headgroup. There are many reports available on the foaming and emulsifying behavior of fatty acids as a function of the pH and ionic strength.[5−8] The first one was published in 1944 by Miles and Ross, who studied the stability of foams produced from fatty acids.[9] Since then, various studies have shown that the fatty acids' bulk self-assemblies can affect the macroscopic properties such as emulsifying and foaming properties.[10−17] From these studies, lamellar phases or vesicles seem to be the most efficient self-assembled structures to stabilize foams and emulsions in contrast to spherical micelles.[14,18,19] The foam stability for fatty acid soaps would be linked to the size of the self-assembled structures as already highlighted in the case of protein aggregates.[20,21] Recently, Stubenrauch et al. pointed out that when surfactants have a polar headgroup with a hydrogen bond donor and a proton acceptor, stable foams can only be generated when hydrogen bonds can be formed between the headgroups at the interface.[22−24] Until now, most of the studies on fatty acid systems have been performed by only looking at the self-assembled structure in bulk or at the interfacial properties to try to understand the mechanisms that drive the destabilization of foam. A global multiscale study needs to be performed at all relevant scales of the system from the molecular scale to the macroscopic scale to increase our understanding on these destabilization phenomena. The question related to the main parameters governing foam stability concerns not only the fatty acid soap systems, but more widely all the surfactant systems

Received: July 5, 2018
Revised: August 26, 2018
Published: August 27, 2018

DOI: 10.1021/acs.langmuir.8b02261
Langmuir 2018, 34, 11076−11085

and remains an open question for the foam community.[20,25−28] For instance, Ferreira et al. have studied recently these issues for a catanionic surfactant system, and have shown that the self-assembled structure in bulk was not the relevant parameter to predict the foam stability.[29]

In this study, our goal was to fully characterize a model fatty acid soap system at the molecular scale, at the scale of the air/water interface, and finally at the mesoscopic scale of the self-assembled structures inside the foam liquid channels, in order to highlight the main parameters governing the foam stability at the macroscopic scale. To achieve this goal, we first selected a model fatty acid soap system already described in a previous work showing a broad polymorphism in bulk: myristic acid dispersed in aqueous solution by using choline hydroxide as counterion.[30] Choline is a quaternary ammonium ion of biological origin, which is physiologically and environmentally harmless, and is very efficient to disperse fatty acids.[31−34] In this model system, the self-assembly in bulk is widely tuned by the molar ratio R, which modifies the pH of the aqueous solution. By tuning R, we modify the quantity of hydroxide ions in bulk. Thus, an increase of R leads to a pH increase due to the addition of hydroxide ions with the choline cation. R sets the pH of the aqueous solution, which in turns governs the ionization state of the fatty acids and the headgroup interactions leading to the broad polymorphism in bulk. In fatty acid systems, different studies have clearly evidenced the effect of the molar ratio in bulk.[1,35−41] For the myristic acid/choline hydroxide system, faceted vesicles, unilamellar and multilamellar vesicles, lamellar phases, and spherical micelles have been observed as a function of R.

In order to investigate the correlation between the bulk self-assembly, the variation of the interfacial properties and of the foam properties as a function of R, we performed a multiscale study by combining experiments and techniques at different length scales to explain the macroscopic foaming properties, and especially foam stability. The aggregated structures confined inside the foam liquid channels were investigated using small angle neutron scattering. The surface properties were determined by coupling surface tension and neutron reflectivity measurements.

MATERIALS AND METHODS

Sample Preparation. The two main components were purchased from Sigma-Aldrich and were used as received: myristic acid (purity > 99%) and choline hydroxide (46 wt % in water). To prepare the myristic acid dispersion in the presence of the choline hydroxide, we first weighed the fatty acid powder to which ultrapure water was added to reach the final concentration fixed at 4.4×10^{-2} mol L^{-1}, which corresponds to 1% weight in water. In the second step, we prepared the choline hydroxide solution at 1 mol·L^{-1} in ultrapure water. Then, this counterion solution was added to reach the desired molar ratio defined as $R = n_{\text{cholinehydroxide}}/ n_{\text{myristicacid}}$ with n the molar concentration in mol L^{-1}. In this study, the concentration of myristic acid was kept at 4.4×10^{-2} mol L^{-1} and only the concentration of counterion was modified to vary R. To fully disperse the fatty acid powder in water in the presence of the counterion, the mixture was heated to 75 °C during 5 min and then cooled down to room temperature before being frozen at −18 °C. This cycle was repeated at least two times to ensure the complete dispersion of the fatty acid powder. All the samples were stored at − 18 °C. Before performing any experiment of characterization, all samples were heated again at 75 °C during 5 min and cooled to room temperature.

Foam Production and Determination of Drainage Kinetics. The foams were produced by two techniques: hand-shaking and gas bubbling. Measurements were performed at 15 °C, 25 and 35 °C and were carried out three times for reproducibility.

In the first method, the foams were produced by vigorous hand-shaking of cylindrical graduated plastic containers of 15 mL (15 mm internal diameter, 118 mm height) filled with 4 mL of fatty acid dispersion. The mixture was agitated for 60 s and all foam samples were produced by the same operator. The evolution of the foam volume was evaluated by naked eye and measured using the graduation of the containers. Second, we also produced foams by bubbling gas into the fatty acid solution using a Foamscan (I.T.Concept, France). Foams were generated in a glass column 21 mm in diameter by bubbling nitrogen gas through a porous glass disc with a 10−16 μm pore size and a diameter of 3 mm. The gas flow rate was fixed at 45 mL·min^{-1}. The final foam volume was fixed at 45 mL. Once this foam volume was reached, the gas flow stopped automatically. A camera recorded pictures of foams every 100 s. The foam formation and stability was monitored by image analysis. To quantify the volume of liquid drained out of the foam at the bottom of the column, conductivity measurements were performed by using electrodes. Before measurements, solutions of myristic acid and choline were introduced inside the glass column and left for 30 min to equilibrate to the required temperature before producing the foam.

Small Angle Neutron Scattering (SANS). We performed SANS experiments on the PACE spectrometer at the Laboratoire Léon Brillouin (Saclay, France). We chose three configurations with a significant overlap between them to get a Q-range spanning from 5×10^{-3} to 3×10^{-1} $Å^{-1}$ (respectively 5 Å at 1 m, 5 Å at 4.7 m, and 13 Å at 4.7 m). The temperature was controlled within ±0.2 °C. The neutron wavelength was set to the desired value with a mechanical velocity selector ($\Delta\lambda/\lambda \approx 0.1$). Standard procedures were applied by the PASINET software to correct the averaged spectra for empty quartz cell, background noise, and detector efficiency contributions in order to obtain scattering in cm^{-1}. The incoherent scattering from solvent was then subtracted afterward.[42]

In order to ensure a good contrast between the fatty acids and the solvent, as well as good contrast between air and solvent in experiments with foams, the dispersions were made in deuterated water (D_2O) as solvent.[43] To study foams by SANS, we produced the foam by using two 10 mL syringes connected by a plastic tube junction.[44] The first syringe contained 5 mL of the initial fatty acid/choline hydroxide dispersion prepared with D_2O and the second was filled with 3 mL of air. Foams were produced by pushing alternatively the plungers of both syringes several times.

The foams were left to drain during 5 min and the drained liquid was collected into a flat quartz cells. The drained foams were put in a flat quartz cells with a 2 mm optical path length by using a needle to introduce carefully the foam inside the cell. A first foam was produced for the measurement at the two configurations corresponding to large and medium Q for which the time acquisition is fast (45 min overall) and a second one similar to the first one was used for measurement at small Q with a longer time of acquisition (60 min). We used this procedure to ensure that the foam evolution was slow on the time-scale of the SANS measurements.

Specular Neutron Reflectivity. Specular neutron reflectivity (SNR) experiments were performed on the horizontal time-of-flight reflectometer EROS at the Laboratoire Léon Brillouin (Saclay, France). The horizontal collimated neutron beam was deflected by a neutron super mirror by an angle of 0.75° on the sample to collect data at a fixed incidence angle of 1.495°. By using a neutron white beam covering wavelength from 3 to 25 Å, it was possible to measure the reflectivity coefficient in a Q-range lying between 5×10^{-3} and 3×10^{-1} $Å^{-1}$. The sample was placed in a sealed cell with two quartz windows allowing the passage of neutrons and avoiding the exchange between D_2O and H_2O from the atmosphere. Measurements were performed at ambient pressure and temperature. The acquisition of the data was recorded for 16 h with slices of 2 h. Samples were prepared by mixing hydrogenated fatty acid and choline hydroxide in deuterated water to ensure a good contrast between the fatty acids and the solvent, and the air−water interfaces and the solvent. The reflectivity curves corresponding to the analytical models presented

DOI: 10.1021/acs.langmuir.8b02261
Langmuir 2018, 34, 11076−11085

within the text were calculated by the optical matrix method with a slicing of the scattering length density profiles in slabs of 10 Å. The experimental resolution of the spectrometer was taken into account in the calculation. The respective calculations of the scattering length density (SLD) of myristic acid molecules and D_2O give $N_b = -0.5 \times 10^{-6}$ Å^{-2} and $N_b = 6.39 \times 10^{-6}$ Å^{-2}.

Surface Tension Measurements. The measurements of the air−solution surface tension as a function of the molar ratio were performed by using the automatized surface tension plate reader Kibron Delta-8 (Kibron, Finland). A volume of 30 μL of dispersions was placed on the 96-hole platform. Measurements were performed at 20 °C after a waiting time of 20 min to ensure equilibrium at the air−water interface for all the samples. Calibration was performed by using ultrapure water at 20 °C. Measurements were performed four times for each sample.

RESULTS

Phase Diagram of the Myristic Acid/Choline Hydroxide System in Bulk as a Function of the Molar Ratio. We first recall the phase diagram of the myristic acid/choline hydroxide system as a function of R and temperature determined in a previous study by coupling SANS and transmission electron microscopy experiments (Figure 1).[30] At low R below 27 °C, faceted vesicles and disks are present. By increasing R, the faceted objects transform into lamellar phases. All these self-assembled structures transit into spherical vesicles above the phase transition close to 27 °C. The transition from faceted vesicles and lamellar phases into spherical vesicles comes from the melting of the alkyl chain.[30] Above the phase transition, the bilayer inside the aggregated structure transits from a gel rigid state to a fluid state. By increasing R, spherical micelles appear in bulk in coexistence with lamellar phases or with vesicles. For $R \geq 0.9$ at all temperatures, only spherical micelles are present in bulk. In this system, by tuning R we modify the pH of the aqueous solution. In bulk, at 20 °C for $0.4 < R \leq 1$, the pH is around 9 close to the pK_a of the myristic acid. For $1 < R < 1.2$, the pH increases from 9 to 11.5, and reaches 12 for $R > 1.3$ (Figure 3).[30] The molar ratio R controls the pH solution, tuning the ionization state of the myristic acid molecules and the interactions between them. It is the modification of both R and temperature in this fatty acid soap system, which leads to these various self-assembled structures in bulk.

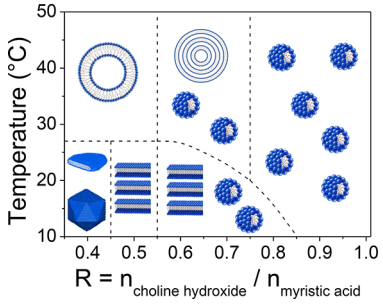

Figure 1. Schematic representation of the phase behavior of the choline hydroxide/myristic acid system in bulk as a function of both R and temperature as determined in a previous study adapted from ref 30.

Self-Assembly Inside the Foam Liquid Channels as a Function of the Molar Ratio. To produce the foams, we have chosen three molar ratios R at 15 °C to be in the presence of three different self-assembled structures in bulk: faceted vesicles (R = 0.4), a mixture between lamellar phases and micelles (R = 0.8) and spherical micelles (R = 1.0).[42] We used SANS experiments to probe the foam and to determine the self-assemblies present inside the foam liquid channels.[43] The scattered intensities for the foams are shown in Figure 2. In order to compare the self-assembly present in the foam with the one in bulk, we plotted also the bulk scattering spectra from which the foams have been made.

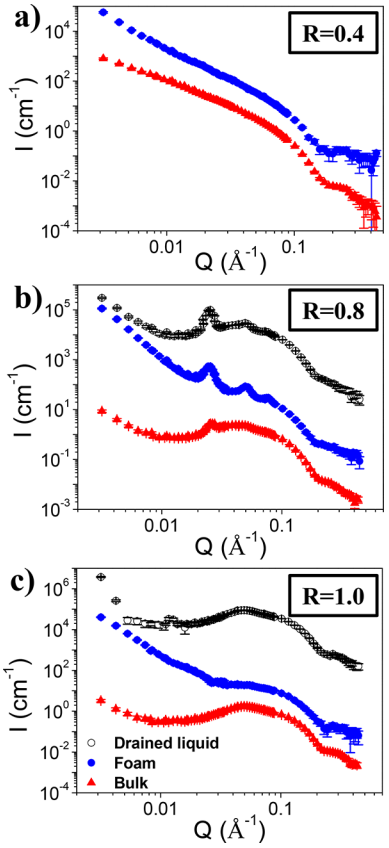

Figure 2. SANS spectra of bulk solutions (red triangle), foams (blue circle), and drained liquid (black empty circle) for (a) R = 0.4, (b) R = 0.8, and (c) R = 1.0. Spectra were shifted in intensity by a factor of 100 from each other for clarity.

First of all, we compared the respective intensities of bulk and foam samples to determine the liquid fraction for the three foams as described recently in the review from Mikhailovskaya et al.[43] For R = 0.4, R = 0.8 and R = 1.0, the liquid fraction were around 22, 24, and 18%, respectively.

At low Q, on the scattering curves for all the foams, a Q^{-4} decay was observed arising from the air−water interfaces of the bubbles and is typical of Porod scattering. The intensity can be described by using, where is the difference of scattering length densities between air and the solvent D_2O and the specific surface corresponding to the amount of gas divided by the water surface per unit volume.[43] By using such equation to fit our data, we determined the average bubble radius (Figure SI.1).[29]

For R = 0.4, R = 0.8 and R = 1.0, the average bubble radii were 62, 56, and 72 μm, respectively. For R = 0.4, from Q = 0.01 to 0.08 Å^{-1}, we observed the same Q^{-2} decay on the SANS spectra of bulk and foams. This Q^{-2} decay corresponds to the presence of bilayers structure. For R = 0.4, faceted

DOI: 10.1021/acs.langmuir.8b02261
Langmuir 2018, 34, 11076−11085

vesicles made of bilayers are present in bulk. Thus, the Q^{-2} decay on the SANS spectra of bulk and foams comes from the scattering of the bilayers of the faceted vesicles. The oscillation at high Q corresponds to the thickness of the bilayers. We observed that it was located at the same position showing that the thickness of the bilayers was the same for the vesicles in bulk and inside the foam liquid channels. The two scattering curves were similar, showing no transformation of the faceted vesicles inside the foam. For R = 0.8, the scattering curve for the bulk corresponds to the mixture of lamellar phases and spherical micelles as described previously.[30] On the scattering curve of the foam, in the middle Q region, we observed three intense sharp peaks located at Q = 0.0255 Å^{-1}, Q = 0.0504 Å^{-1}, and Q = 0.0765 Å^{-1}. Their positions were exactly in a ratio 1:2:3 (Q_0, $2Q_0$, 3 Q_0), which indicates the presence of lamellar phases inside the foam liquid channels. The intensity of the peaks was higher than for the bulk dispersion showing that the quantity of lamellar phases was higher inside the foam than for the bulk dispersion. Three hypotheses could explain this difference: (i) during foam generation, the high shear rates could induce the formation of lamellar phases from the micelles, (ii) during foam generation, the foam could be enriched by lamellar phases, or (iii) during the drainage, only the micelles that have small size and high mobility are drained contrary to the lamellar phases which can stay entrapped inside the foam. In order to rule out the hypotheses, a SANS experiment was carried out on the drained liquid. The scattering curve was very similar to the one obtained for the bulk dispersion showing the coexistence of both spherical micelles and lamellar phases. Therefore, we can conclude that most of the lamellar phases remained entrapped inside the foam, and the spherical micelles were free to drain out of the foam with a small quantity of lamellar phases. For R = 1.0, the bulk dispersion contained only spherical micelles with a diameter around 18 ± 1 Å^{-1}. For both the foam and the drained liquid, we observed that the scattering curves were similar to the one obtained for the bulk, especially at high Q where the form factor is probed showing that the micelle size remained the same. Since micelles were composed by ionized fatty acid molecules, they bear an overall negative charge and repel themselves over large distances due to electrostatic repulsions. This gives rise to a broad correlation peak in the medium Q part. From the position of the peak we can estimate the average distance between spherical micelles. In the bulk, the spherical micelles gave rise to a broad correlation peak at Q = 0.0495 Å, which corresponded to a distance (d) between micelles of around 125 Å ($d = 2\pi/Q$). For the drained solution, the peak position was slightly shifted to lower Q, showing that the mean distance between micelles increased and was around 135 Å, i.e., the number of micelles was lower in the drained solution in comparison to the bulk dispersion. We suppose that this comes from the fact that a large quantity of fatty acids remains inside the foam as monomers adsorbed at the interface, compared to the bulk under where they form micelles.

In summary, these SANS results show that the morphology of the self-assembled nanostructures remained the same during the passage from bulk to foam for the three samples probed.

Effect of the Molar Ratio on the Surface Properties. As our goal was to understand how the foam was stabilized as a function of R, it was mandatory to collect information on how these fatty acid molecules adsorb at the air−water interface. We focused on the surface properties as a function of R by coupling surface tension and specular neutron reflectivity (SNR) measurements.

We measured the evolution of the surface tension as a function of R at room temperature to determine the effect on the surface activity of the myristic acid (Figure 3). For 0.4 < R < 1, the surface tension was around 26 ± 2 mN/m. For 1 ≤ R < 1.2, the surface tension drastically increased from 26 to 45 mN/m. For R > 1.2, the surface tension remained constant around 45 ± 1 mN/m. As a function of R, three regimes of surface tension were determined: low, intermediate, and high surface tension. By comparing with the pH evolution as a function of R determined in a previous study, we observed that the three surface tension regimes followed exactly the evolution of the pH in bulk (Figure 3).[30]

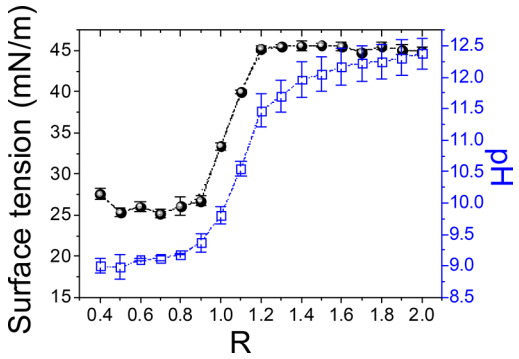

Figure 3. Evolution of surface tension (black circle) and pH (blue square) in choline hydroxide/myristic acid dispersions as a function of molar ratio R at 25 °C.

Beyond surface tension measurements, various interfacial structures have been described in literature for surfactant systems and neutron reflectivity is a powerful technique to determine them at the air/water interface (surfactant monolayers, lamellar phases, multilamellar vesicles and tubes).[45−47] We performed SNR experiments at 20 °C for two molar ratios R containing self-assembled bilayer structures in bulk: R = 0.4 (faceted vesicles) and R = 0.5 (lamellar phases). On the SNR curves, we observed a Q^{-4} scattering decay coming from the pure air/water interface and regular interference fringes showing the presence of a thick layer of myristic acid at the interface (Figures SI.2 and SI.3). To fit the SNR data, we used the multilayer model (see the Supporting Information for the description of data fitting).[45,48] From these results, we can conclude that the faceted vesicles and lamellar phases form a lamellar phase structure at the air−water interface adsorbed below a fatty acid monolayer.

Effect of the Molar Ratio on the Foam Properties. We studied the foam properties (foamability and foam stability) as a function of both R and temperature. The molar ratio was varied from 0.4 to 2.0 and the temperature was fixed at 15 or 35 °C in order to have different self-assemblies in bulk (Figure 4).

First, we produced foams by bubbling nitrogen gas into each fatty acid dispersions allowing a quantitative description in terms of foamability (how much foam is produced) and foam stability (how the foam evolves). At all temperatures, the foams were formed quickly in around 60 ± 5 s and were made of small homogeneous bubbles (in the range of 50−100 μm) (Table SI.1 and Figure SI.4). Only for R > 1.5, we observed a slight increase of the time needed to reach the fixed foam

DOI: 10.1021/acs.langmuir.8b02261
Langmuir 2018, 34, 11076−11085

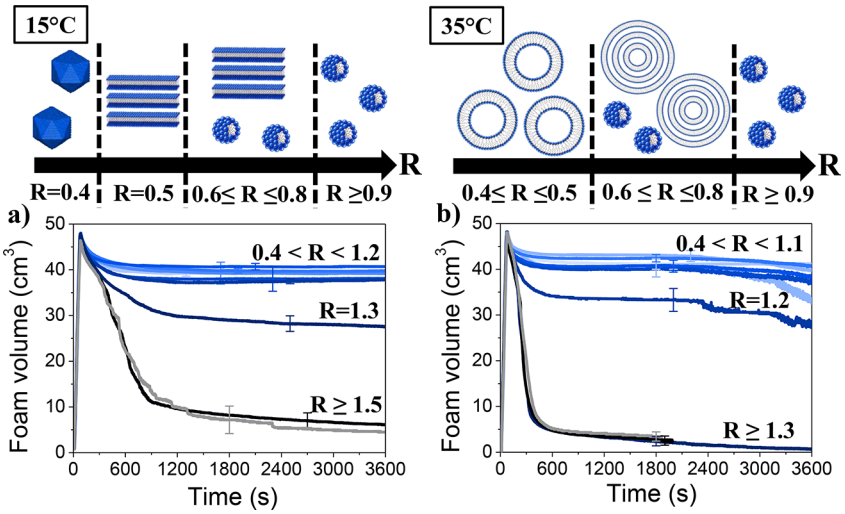

Figure 4. Evolution of the foam volume as a function of time for foams produced by bubbling gas for various molar ratios (R) at two temperatures: (a) 15 °C and (b)35 °C. The schematic drawings represent the self-assemblies present in bulk as a function of both R and temperature as determined in a previous study.[30]

volume. Therefore, the foamability was high whatever the R since all the gas was encapsulated in the foam at the end of bubbling, with no influence of the self-assembly structure.

To obtain information on the foam stability, we recorded the evolution of the foam volume as a function of time (Figure 4). First, at 15 °C, for $0.4 < R < 1.2$, the foam volume was constant during 3600 s around 40 cm^3 (Figure 4.a). These foams can be denoted as stable foams. For $R = 1.3$, the foam volume decreased slowly to reach 30 cm^3 after 3600 s. This foam had an intermediate stability. For $R \geq 1.5$, the foam volume decreased quickly with time. At the end of the experiment, only few bubbles remained inside the foam column. These foams are classified as unstable foams. We observed three regimes as a function of R (Figure 4a). At 25 °C, the self-assemblies are the same as at 15 °C in bulk and the same evolution of foam stability was observed (Figure SI.5). At 35 °C, three regimes were also obtained (Figure 4b). For $0.4 < R < 1.1$, stable foams were observed with a constant foam volume around 40 cm^3 during 3600 s. For $R = 1.2$, the foam had an intermediate stability with a foam volume which decreased slowly with time. For $R \geq 1.3$, the foams were unstable with a fast foam volume decrease with time. At all temperatures, three regimes of foam stability were observed and we classified them as stable foam, intermediate stability and unstable foams. Only the limits between the regimes were slightly shifted to lower R by increasing the temperature. Moreover, the foams were a little less stable at 35 °C since the foams started to break up at the top after 2400 s, while nothing happened for the foams at 15 and 25 °C.

We also measured the evolution of the amount of liquid inside the foam with time to follow the drainage (Figure SI.6). After foam formation for all R and temperatures, the liquid fraction was high around 20 ± 5%. No trend for the liquid fraction was observed as a function of R. The liquid fraction quickly decreased with time for all samples, showing that drainage occurred whatever the R. However, we observed that the drainage rate was faster at 35 °C than at 15 °C at $R < 1$. The liquid fraction decreased faster for $R \geq 1$ for all temperatures.

It is known in the literature that the foam production method influences the foaming properties.[44] For comparison, we also produced foams by hand-shaking (Figure 5).The advantage of shaking is that it can be performed in closed bottles, which permit us to follow the evolution of the foam volume over longer times, 24 h in our case. Moreover, the use of two different foaming techniques leads to different bubble sizes as well as liquid fractions at the end of the foam production. Hand-shaking was used to confirm the observations made from the bubbling techniques *i.e.* the three foam stability regimes. After foam formation for all R and temperatures, the liquid fraction was high around 30 ± 5%, for all R and temperatures. The bubble diameters generated with the handshaking method were larger than with the bubbling method (around 50−100 μm for bubbling and around 150 μm for handshaking).

At 15 °C, we obtained again three regimes of foam stability (Figure 5a). For $0.4 < R \leq 1.1$, the foam volume slightly decreased after 24 h of conservation of the foam at 15 °C. For $R = 1.1$, after 24 h, the foam volume decreased from around 12 to 3 cm^3, and the bubble size increased as seen by the naked eye. For $R \geq 1.3$, there was almost no more foam after only 1 h. At 35 °C, whatever the R, there was no more foam after 24 h (Figure 5b). After 5 h, three regimes of foam stability were again observed. For $0.4 < R \leq 1$, the foams were stable with a foam volume decrease of only few cm^3 after 5 h of conservation of the foam. For $R = 1.1$, after 5 h, the foam had an intermediate stability since the foam volume decreased from around 12 to 3 cm^3 accompanied by an increase of the bubbles size. For $R \geq 1.2$, the foams were unstable with no more foam after only 1 h; only few very big bubbles remained present inside the plastic tube. The same trend was observed at 25 °C, stable foams for $0.4 < R < 1$, intermediate stability for $1 \leq R \leq 1.1$, and unstable foams for $R \geq 1.2$ (Figure SI.7).

Between the two foaming methods, we observed that the results were quite close and three main regimes were distinguished for the evolution of the foam volume over time as a function of R. However, the onset of the transition between stable foams and intermediate stability was shifted to lower R values in the case of foams produced by handshaking in comparison to foams produced by bubbling, a trend that was observed for all temperatures. This shows that the initial

DOI: 10.1021/acs.langmuir.8b02261
Langmuir 2018, 34, 11076−11085

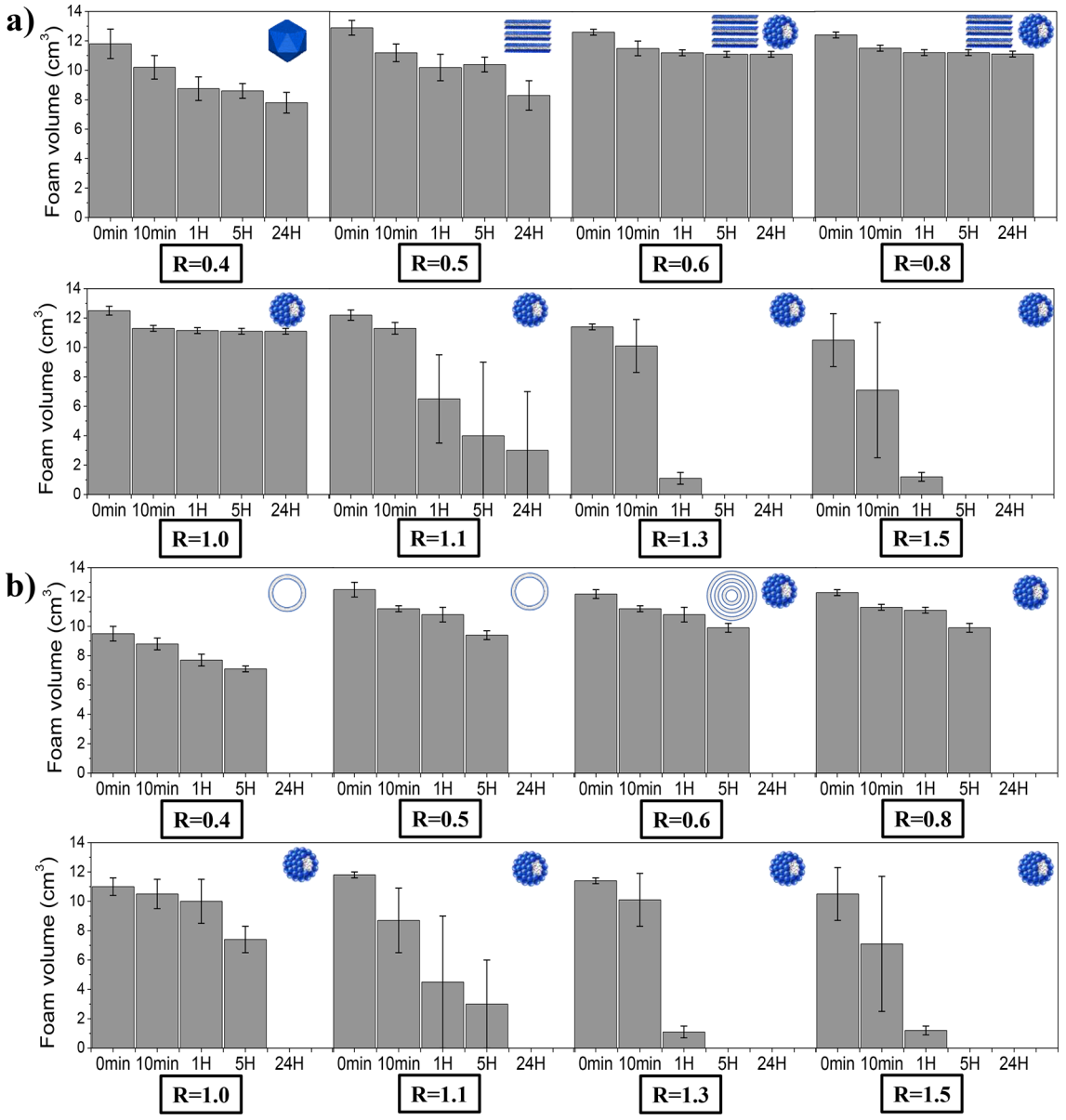

Figure 5. Evolution of the foam volume as a function of time for foams produced by hand-shaking for various molar ratios (R) at two temperatures: (a) 15 °C and (b) 35 °C. The schematics represent the self-assemblies present in bulk as a function of both R and the temperature.

bubbles size and liquid fraction had a slight effect on the R threshold values between the three regimes.

DISCUSSION

Links between Self-Assembly in Bulk, Interfacial, and Foam Properties as a Function of *R*. The results we have gathered at all the different scales from the molecular to the macroscopic scale show that (i) three different regimes of surface tension were observed, which are strongly linked to R and therefore to pH; (ii) the foamability does not depend on R; (iii) the foam stability is tuned by R and three regimes of foam stability are obtained (high, medium, and low); (iv) inside the foam liquid channels, the structure of the self-assembled nanostructures are identical to those in bulk and are tuned by R. This combination of results should allow us to depict the mechanisms that lead to the three foam stability regimes observed by addressing the following questions: Does it come from changes of the bulk or interfacial properties, or both? Is the foam stability driven by the bulk or the interfacial properties? What sets the transitions between high, medium and low foam stability regimes?

It is well-known that the destabilization of foams occurs due to three main mechanisms: coalescence, coarsening, and drainage.[25,49,50] Here, we observed that the foam drainage was slightly slower in the presence of self-assembled bilayer structures than in the presence of spherical micelles. This difference in drainage rate comes from a much higher bulk viscosity for the dispersions containing vesicles, lamellar phases, and so forth than for spherical micelles (Figure SI.8).[51,52] However, even in the case of foams produced at low R containing micrometer-size aggregates, the foam drainage occurred leading to relatively dry foams after less than 1 h for foams produced by bubbling (liquid fraction below 5%), even if such foams show a very good stability. Therefore, the foam stability was mainly linked to coalescence and coarsening phenomena in our model system, and not to the drainage.

DOI: 10.1021/acs.langmuir.8b02261
Langmuir 2018, 34, 11076−11085

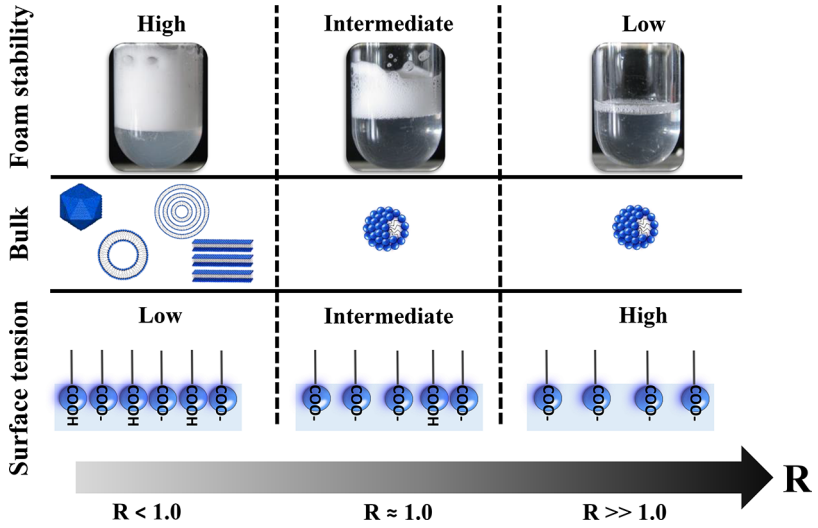

Figure 6. Schematic illustrating the links between molar ratio (R), foam stability, bulk self-assembly, and surface properties.

To limit the coalescence and coarsening phenomena, the mechanical properties of the interfacial layers such as the resistance to the compression and the elasticity are important. In the literature, it is described that the surface properties are linked to the ionization state of the fatty acid molecules in bulk, which is controlled by the pH.[25,50] For fatty acid monolayers, the difference in pK_a between the surface and the bulk is small. When the pH is close to the pK_a, the fatty acids are present both under protonated and deprotonated states in 1:1 proportion in bulk.[5,6,53]

In our system, for $0.4 < R \leq 1$, low surface tensions were obtained. The pH in bulk was around 9 corresponding to the pK_a of the myristic acid. Based on the results obtained in similar systems in the literature, we can suppose that at the air/water interface, protonated and deprotonated molecules under ionized state are both present.[7,54,55] We suppose that there is a synergistic adsorption of both molecular species and they interact by hydrogen bonding, causing a reduction of the intermolecular distance leading to a dense monolayer at the interface. In the literature, it is known that the presence of carboxylic group at the interface decreases the electrostatic repulsive forces leading to a tighter monolayer packing.[7,54,55] This dense monolayer formed by both species at the interface gives rise to an elastic surfactant layer as highlighted in similar systems.[22−24] When the pH in bulk increases by increasing R, the protonated myristic acid molecules progressively become deprotonated. At the interface, the ratio of deprotonated molecules to protonated in the monolayer increases, which increases the electrostatic repulsions between the charged carboxylate headgoups. This reduces the density of fatty acids that can be adsorbed compared to what happens at lower R. Consequently, for $1 < R < 1.2$ the surface tension increases progressively in accordance to the decrease of fatty acids surface density. For $R > 1.3$ corresponding to high pH, only deprotonated molecules are present both in bulk and at the interface. The strong repulsive forces between the carboxylate headgroups are maximal and the adsorption density is minimal and lower than at pH close to the pK_a (Figure 6).[56] In such range of R, the surface tension reaches its highest values due to low density of fatty acid molecules at the interface. Similar results have been described in the literature for sodium salt of myristic acid by coupling surface tension and Infrared Absorption Spectroscopy.[54] Thus, three different ranges of surface tension exist as a function of R: low for $R < 1$, intermediate for $R \approx 1$ and high for $R \gg 1$ (Figure 6). The intermediate regime corresponds to the transition between the low surface tension regime to the high surface tension regime due to the progressive deprotonation of the fatty acid molecules. The transition between these two extremes is smooth.

It has recently been suggested that the ability of surfactants to form hydrogen bonds at the interface tunes the stability of foam films and therefore to the overall stability of the foam at the macroscopic scale.[24] Since we have identified on our model system three ranges of R for the surface tension, we can discuss their respective influences on three different regimes of foam stability identified as a function of R: high for $R < 1$, intermediate for $R \approx 1$ and low for $R \gg 1$ (Figure 6).

High Foam Stability Regime for *R* below Equimolarity. For this high foam stability regime, all the dispersions contained large self-assembled bilayer structures (faceted vesicles, spherical vesicles and lamellar phases) both in bulk and in the foam liquid channels. This high foam stability regime corresponds to the low surface tension regime where a dense monolayer is formed at the interface, which ensures a good protection for the bubbles against coarsening and coalescence. Moreover, we have shown by SNR that, below this fatty acid monolayer, the faceted vesicles and lamellar phases were adsorbed and formed multilamellar phases at the interface. These structures form thick interface layers, and are known to reinforce the protection of the bubbles since the coarsening is linked to the permeability of the interfacial layer.[57−59]

Low Foam Stability Regime for *R* above Equimolarity. The foams obtained from dispersions containing spherical micelles for $R \gg 1$ were destroyed quickly with time. We showed that only spherical micelles were present inside the foam liquid channels, which does not reduce drainage due to the low bulk viscosity. This low foam stability regime corresponds also to the high surface tension regime with a monolayer that contains only a low density of fatty acid molecules and cannot protect the bubbles against coalescence and coarsening. The mechanisms of foam destabilization are not blocked resulting in unstable foams.

DOI: 10.1021/acs.langmuir.8b02261
Langmuir 2018, 34, 11076−11085

In this high regime of *R*, a large excess of counterions in the foam can affect also its foamability. In this regime, the thin film stability is due to electrostatic repulsion between the ionic double layers associated with the adsorbed ionic surfactants on the two sides of the liquid film. A large addition of choline hydroxide as counterion screens these interactions and in turn causes the shortening of the electrical double layers, decreasing the stability of the foam. This fast foam destabilization could also explain why the foamability is lower than for the other *R* regimes; as destabilization already took place during the foam formation.[60] This phenomenon has been already described for mixtures between cationic surfactants and organic counterions.[61,62]

Intermediate Foam Stability Regime for *R* Close to the Equimolarity. Our results show that, in the vicinity of equimolarity, foams were relatively stable even though only micelles were detected in the bulk foam channels as for the low foam stability regime. This is a proof that the conditions required to obtain stable foams are not only driven by the presence of large self-assembled structures in bulk (vesicles, lamellar phases, etc.), but also to the strong influence of the packing of fatty acids at the surface. This intermediate regime is a smooth crossover between the two extreme regimes (high and low foam stability). For this intermediate foam stability regime, the surface tension regime also corresponds to the crossover range of surface packing and surface tension between high and low surface tension. The result at the macroscopic scale is an intermediate foam stability.

Effect of the Alkyl Chain Melting on the Phase Behavior and Foam Stability. In this system, the alkyl chain melting occurs around 27 °C, which has been shown to induce a change in the rigidity of the self-assemblies in bulk from faceted vesicles and lamellar phases to spherical vesicles.[30] The melting has rather a low influence on the foam stability, as shown by the results obtained below (15 and 25 °C), and above the alkyl chain melting temperature (35 °C). Indeed, the general foam stability trend was not influenced by the state of the chains and for all temperatures, three regimes of foam stability were always observed. However, above 27 °C, the foam stability was lower than below. This transition at the molecular scale mainly modifies the properties of the interfacial layer, where the molten chains are more mobile, less well packed, and have lower resistance to deformation. Therefore, they are less able to resist against coalescence and coarsening and lead to a decrease in the foam stability.

CONCLUSION

In this study, we demonstrated that it is possible to adjust the foam stability of a system of fatty acids at the macroscopic scale by tuning a simple parameter, the molar ratio *R* between the myristic acid and its organic counterion the choline hydroxide. Indeed, the tuning of *R* induces changes at the molecular scale, which impact at the same time the surface properties, and the self-assembly in the foam liquid channels at the microscopic scale. *R* is a simple trigger to tune the foam stability from low to high (Figure 6). By using a multiscale approach, we highlighted that the foam stability could not be explained only by looking at the size and nature of the self-assembly present in bulk, contrary to results described in previous studies in similar fatty acid/organic counterion systems.[16,18] Indeed, we observed either relatively stable foam (close to equimolarity) or unstable foam (above equimolarity) in the presence of the same self-assembly: spherical micelles. Our results confirm recent conclusions obtained by Ferreira et al., for catanionic systems, showing that the self-assembly structure is not the only appropriate parameter to predict foam stability.[29]

The difference of foam stability in our system is mainly linked to the properties of the fatty acid monolayer at the interface, which depends on the ionization state of the myristic acid. By controlling the molar ratio *R*, we can set the pH of the bulk, which is linked to the quantity of hydroxide ions introduced by the choline hydroxide counterion. The pH governs the ratio between the deprotonated and protonated molecules both in bulk and at the interface, and also the interactions between them: hydrogen bonding and/or repulsive electrostatic interactions. The surface tension and the density of fatty acids at the interface are directly linked to *R*. Therefore, we can suppose that the foam stability follows mainly the variation of the interfacial properties governed by *R*, which plays a crucial role at the molecular scale. This result can be explained by the fact that we are dealing with coalescence and coarsening issues in this system. These foam destabilization mechanisms are happening at the scale of the thin films separating bubbles, which are made of two interfaces in interaction. For fatty acid soap systems, the main requirement to obtain stable foam is to stabilize the bubbles by having a mixture of protonated and deprotonated molecules at the interface interacting by hydrogen bonds giving rise to a dense and elastic surfactant layer counteracting coalescence and coarsening.

Our results seem to be confirming the role of intermolecular hydrogen bonds between surfactant head groups on the foam stability, as demonstrated recently with other types of surfactants.[22−24] One of the next steps of our study is to confirm the results obtained with myristic acid by using other counterions as already described in the literature in the bulk and with other surfactants enable to form hydrogen bonding.[63−65]

This study based on a fatty acid soap system provides new insights to understand the relationships existing between foam stability and self-assembly, which is of interest to all the scientists working on formulation, foam, and self-assembly, and will stimulate further works on the subject. From an applied point of view, this study could help to improve the foaming formulations based on fatty acid soaps for various applications in detergency, cosmetics, and so forth.

ASSOCIATED CONTENT

Supporting Information

The Supporting Information is available free of charge on the ACS Publications website at DOI: 10.1021/acs.langmuir.8b02261.

SANS spectra; SNR curves; comparison of SNR results; evolution of foam volume as a function of time; evolution of viscoscity as a function of shear rate (PDF)

AUTHOR INFORMATION

Corresponding Author

*E-mail: anne-laure.fameau@nantes.inra.fr.

ORCID

Fabrice Cousin: 0000-0001-7523-5160
Anniina Salonen: 0000-0002-8286-3250
Anne-Laure Fameau: 0000-0002-8237-2216

DOI: 10.1021/acs.langmuir.8b02261
Langmuir 2018, 34, 11076−11085

Notes

The authors declare no competing financial interest.

■ ACKNOWLEDGMENTS

A.A. would like to thank the region Pays de la Loire and INRA for the allocation of her Ph.D. grant. The beam time allocation on both the spectrometer PACE and on the reflectometer EROS from the Laboratoire Léon Brillouin was gratefully appreciated. The authors would like to thank Dr. Marc Anton for the useful discussions. The experimental assistance of B. Houinsou-Houssou was greatly appreciated.

■ REFERENCES

(1) Fameau, A.-L.; Zemb, T. Self-assembly of fatty acids in the presence of amines and cationic components. *Adv. Colloid Interface Sci.* **2014**, *207*, 43−64.

(2) Wolfrum, S.; Marcus, J.; Touraud, D.; Kunz, W. A renaissance of soaps?—How to make clear and stable solutions at neutral pH and room temperature. *Adv. Colloid Interface Sci.* **2016**, *236*, 28−42.

(3) Johansson, I.; Svensson, M. Surfactants based on fatty acids and other natural hydrophobes. *Curr. Opin. Colloid Interface Sci.* **2001**, *6* (2), 178−188.

(4) Chupa, J.; Misner, S.; Sachdev, A.; Wisniewski, P.; Smith, G. A. Soap, Fatty Acids, and Synthetic Detergents. In *Handbook of Industrial Chemistry and Biotechnology*; Springer, 2012; pp 1431−1471.

(5) Kanicky, J. R.; Poniatowski, A. F.; Mehta, N. R.; Shah, D. O. Cooperativity among molecules at interfaces in relation to various technological processes: Effect of chain length on the pK(a) of fatty acid salt solutions. *Langmuir* **2000**, *16* (1), 172−177.

(6) Theander, K.; Pugh, R. J. Synergism and foaming properties in mixed nonionic/fatty acid soap surfactant systems. *J. Colloid Interface Sci.* **2003**, *267* (1), 9−17.

(7) Golemanov, K.; Denkov, N. D.; Tcholakova, S.; Vethamuthu, M.; Lips, A. Surfactant mixtures for control of bubble surface mobility in foam studies. *Langmuir* **2008**, *24* (18), 9956−9961.

(8) Zhang, Y.; Kong, W.; An, P.; He, S.; Liu, X. CO_2/pH-Controllable Viscoelastic Nanostructured Fluid Based on Stearic Acid Soap and Bola-Type Quaternary Ammonium Salt. *Langmuir* **2016**, *32* (10), 2311−2320.

(9) Miles, G. D.; Ross, J. Foam Stability of Solutions of Soaps of Pure Fatty Acids. *J. Phys. Chem.* **1944**, *48* (5), 280−290.

(10) Fameau, A.-L.; Houinsou-Houssou, B.; Ventureira, J.; Navailles, L.; Nallet, F.; Novales, B.; Douliez, J.-P. Self-Assembly, Foaming, and Emulsifying Properties of Sodium Alkyl Carboxylate/Guanidine Hydrochloride Aqueous Mixtures. *Langmuir* **2011**, *27* (8), 4505−4513.

(11) Fameau, A.-L.; Saint-Jalmes, A.; Cousin, F.; Houssou, B. H.; Novales, B.; Navailles, L.; Nallet, F.; Gaillard, C.; Boue, F.; Douliez, J.-P. Smart Foams: Switching Reversibly between Ultrastable and Unstable Foams. *Angew. Chem., Int. Ed.* **2011**, *50* (36), 8264−8269.

(12) Fameau, A.-L.; Ventureira, J.; Novales, B.; Douliez, J.-P. Foaming and emulsifying properties of fatty acids neutralized by tetrabutylammonium hydroxide. *Colloids Surf., A* **2012**, *403*, 87−95.

(13) Fameau, A.-L.; Gaillard, C.; Marion, D.; Bakan, B. Interfacial properties of functionalized assemblies of hydroxy-fatty acid salts isolated from fruit tomato peels. *Green Chem.* **2013**, *15* (2), 341−346.

(14) Xu, W.; Gu, H.; Zhu, X.; Zhong, Y.; Jiang, L.; Xu, M.; Song, A.; Hao, J. CO2-controllable foaming and emulsification properties of the stearic acid soap systems. *Langmuir* **2015**, *31* (21), 5758−5766.

(15) Shu, X.; Meng, Y.; Wan, L.; Li, G.; Yang, M.; Jin, W. pH-Responsive Aqueous Foams of Oleic Acid/Oleate Solution. *J. Dispersion Sci. Technol.* **2014**, *35*, 293.

(16) Novales, B.; Riaublanc, A.; Navailles, L.; Houssou, B. H.; Gaillard, C.; Nallet, F.; Douliez, J. P. Self-Assembly and Foaming Properties of Fatty Acid-Lysine Aqueous Dispersions. *Langmuir* **2010**, *26* (8), 5329−5334.

(17) Li, G.; Yang, Q.; Song, A.; Hao, J. Self-assembled structural transition from vesicle phase to sponge phase and emulsifying properties in mixtures of arginine and fatty acids. *Colloids Surf., A* **2015**, *487*, 198−206.

(18) Novales, B.; Navailles, L.; Axelos, M.; Nallet, F.; Douliez, J. P. Self-assembly of fatty acids and hydroxyl derivative salts. *Langmuir* **2008**, *24* (1), 62−68.

(19) Xu, W.; Liu, H.; Song, A.; Hao, J. Bilayers and wormlike micelles at high pH in fatty acid soap systems. *J. Colloid Interface Sci.* **2016**, *465*, 304−310.

(20) Fameau, A.-L.; Salonen, A. Effect of particles and aggregated structures on the foam stability and aging. *C. R. Phys.* **2014**, *15*, 748.

(21) Douliez, J.-P.; Gaillard, C. Self-assembly of fatty acids: from foams to protocell vesicles. *New J. Chem.* **2014**, *38* (11), 5142−5148.

(22) Ranieri, D.; Preisig, N.; Stubenrauch, C. On the Influence of Intersurfactant H-Bonds on Foam Stability: A Study with Technical Grade Surfactants. *Tenside, Surfactants, Deterg.* **2018**, *55* (1), 6−16.

(23) Schellmann, K.; Preisig, N.; Claesson, P.; Stubenrauch, C. Effects of protonation on foaming properties of dodecyldimethylamine oxide solutions: a pH-study. *Soft Matter* **2015**, *11* (3), 561−571.

(24) Stubenrauch, C.; Hamann, M.; Preisig, N.; Chauhan, V.; Bordes, R. On how hydrogen bonds affect foam stability. *Adv. Colloid Interface Sci.* **2017**, *247*, 435−443.

(25) Pugh, R. J. *Bubble and foam chemistry*; Cambridge University Press: 2016.

(26) Fauser, H.; Uhlig, M.; Miller, R.; Klitzing, R. V. Surface adsorption of oppositely charged SDS: C12TAB mixtures and the relation to foam film formation and stability. *J. Phys. Chem. B* **2015**, *119* (40), 12877−12886.

(27) Langevin, D. Influence of interfacial rheology on foam and emulsion properties. *Adv. Colloid Interface Sci.* **2000**, *88* (1), 209−222.

(28) Prud'homme, R. *Foams: Theory: Measurements: Applications*; Routledge: 2017.

(29) Ferreira, J.; Mikhailovskaya, A.; Chennevière, A.; Restagno, F.; Cousin, F.; Muller, F.; Degrouard, J.; Salonen, A.; Marques, E. F. Interplay between Bulk Self-Assembly, Interfacial and Foaming Properties in a Catanionic Surfactant Mixture of Varying Composition. *Soft Matter* **2017**, *13*, 7197.

(30) Arnould, A.; Perez, A. A.; Gaillard, C.; Douliez, J.-P.; Cousin, F.; Santiago, L. G.; Zemb, T.; Anton, M.; Fameau, A.-L. Self-assembly of myristic acid in the presence of choline hydroxide: Effect of molar ratio and temperature. *J. Colloid Interface Sci.* **2015**, *445*, 285−293.

(31) Klein, R.; Touraud, D.; Kunz, W. Choline carboxylate surfactants: biocompatible and highly soluble in water. *Green Chem.* **2008**, *10* (4), 433−435.

(32) Klein, R.; Kellermeier, M.; Drechsler, M.; Touraud, D.; Kunz, W. Solubilisation of stearic acid by the organic base choline hydroxide. *Colloids Surf., A* **2009**, *338* (1−3), 129−134.

(33) Klein, R.; Tiddy, G. J.; Maurer, E.; Touraud, D.; Esquena, J.; Tache, O.; Kunz, W. Aqueous phase behaviour of choline carboxylate surfactants—exceptional variety and extent of cubic phases. *Soft Matter* **2011**, *7* (15), 6973−6983.

(34) Wei, Y.; Wang, H.; Liu, G.; Wang, Z.; Yuan, S. A molecular dynamics study on two promising green surfactant micelles of choline dodecyl sulfate and laurate. *RSC Adv.* **2016**, *6* (87), 84090−84097.

(35) Li, G.; Liu, Y.; Xu, W.; Song, A.; Hao, J. Transition of phase structures in mixtures of lysine and fatty acids. *J. Phys. Chem. B* **2014**, *118* (51), 14843−14851.

(36) Dubois, M.; Demé, B.; Gulik-Krzywicki, T.; Dedieu, J.-C.; Vautrin, C.; Désert, S.; Perez, E.; Zemb, T. Self-assembly of regular hollow icosahedra in salt-free catanionic solutions. *Nature* **2001**, *411* (6838), 672−675.

(37) Zemb, T.; Dubois, M.; Deme, B.; Gulik-Krzywicki, T. Self-assembly of flat nanodiscs in salt-free catanionic surfactant solutions. *Science* **1999**, *283* (5403), 816−819.

(38) Zana, R. Partial phase behavior and micellar properties of tetrabutylammonium salts of fatty acids: Unusual solubility in water and formation of unexpectedly small micelles. *Langmuir* **2004**, *20* (14), 5666−5668.

DOI: 10.1021/acs.langmuir.8b02261
Langmuir 2018, 34, 11076−11085

(39) Zana, R.; Schmidt, J.; Talmon, Y. Tetrabutylammonium alkyl carboxylate surfactants in aqueous solution: Self-association behavior, solution nanostructure, and comparison with tetrabutylammonium alkyl sulfate surfactants. *Langmuir* **2005**, *21* (25), 11628−11636.
(40) Wang, Y.; Jiang, L.; Shen, Q.; Shen, J.; Han, Y.; Zhang, H. Investigation on the self-assembled behaviors of C 18 unsaturated fatty acids in arginine aqueous solution. *RSC Adv.* **2017**, *7* (66), 41561−41572.
(41) Fan, Y.; Ma, J.; Fang, Y.; Liu, T.; Hu, X.; Xia, Y. Neutral and acid-adapted fatty acid vesicles of conjugated linoleic acid. *Colloids Surf., B* **2018**, *167*, 385−391.
(42) Brûlet, A.; Lairez, D.; Lapp, A.; Cotton, J.-P. Improvement of data treatment in small-angle neutron scattering. *J. Appl. Crystallogr.* **2007**, *40* (1), 165−177.
(43) Mikhailovskaya, A.; Zhang, L.; Cousin, F.; Boué, F.; Yazhgur, P.; Muller, F.; Gay, C.; Salonen, A. Probing foam with neutrons. *Adv. Colloid Interface Sci.* **2017**, *247*, 444−453.
(44) Drenckhan, W.; Saint-Jalmes, A. The science of foaming. *Adv. Colloid Interface Sci.* **2015**, *222*, 228−259.
(45) Penfold, J.; Thomas, R. K. Neutron reflectivity and small angle neutron scattering: an introduction and perspective on recent progress. *Curr. Opin. Colloid Interface Sci.* **2014**, *19* (3), 198−206.
(46) Fameau, A.-L.; Douliez, J.-P.; Boue, F.; Ott, F.; Cousin, F. Adsorption of multilamellar tubes with a temperature tunable diameter at the air/water interface. *J. Colloid Interface Sci.* **2011**, *362* (2), 397−405.
(47) Curschellas, C.; Kohlbrecher, J.; Geue, T.; Fischer, P.; Schmitt, B.; Rouvet, M.; Windhab, E. J.; Limbach, H. J. R. Foams Stabilized by Multilamellar Polyglycerol Ester Self-Assemblies. *Langmuir* **2013**, *29* (1), 38−49.
(48) Penfold, J. Neutron scattering for surface characterization. *Curr. Sci.* **2000**, *78* (12), 1458−1466.
(49) Cantat, I.; Cohen-Addad, S.; Elias, F.; Graner, F.; Höhler, R.; Pitois, O.; Rouyer, F.; Saint-Jalmes, A. *Foams: structure and dynamics*; OUP: Oxford, 2013.
(50) Pugh, R. J. Foaming, foam films, antifoaming and defoaming. *Adv. Colloid Interface Sci.* **1996**, *64*, 67−142.
(51) Safouane, M.; Saint-Jalmes, A.; Bergeron, V.; Langevin, D. Viscosity effects in foam drainage: Newtonian and non-newtonian foaming fluids. *Eur. Phys. J. E: Soft Matter Biol. Phys.* **2006**, *19* (2), 195−202.
(52) Stoyanov, S.; Dushkin, C.; Langevin, D.; Weaire, D.; Verbist, G. Effect of the rheology on foam drainage. *Langmuir* **1998**, *14* (16), 4663−4665.
(53) Chen, L.-C.; Wang, H.-P.; Deng, Y.-H.; Deng, S.-P. Vesicle formation by proton transfer driven short-tailed fatty acids of C4−C8 chain length in water. *Soft Matter* **2017**, *13* (6), 1291−1298.
(54) Wen, X. Y.; Lauterbach, J.; Franses, E. I. Surface densities of adsorbed layers of aqueous sodium myristate inferred from surface tension and infrared reflection absorption spectroscopy. *Langmuir* **2000**, *16* (17), 6987−6994.
(55) Yim, K. S.; Rahaii, B.; Fuller, G. G. Surface rheological transitions in Langmuir monolayers of bi-competitive fatty acids. *Langmuir* **2002**, *18* (17), 6597−6601.
(56) Coltharp, K. A.; Franses, E. I. Equilibrium and dynamic surface tension behavior of aqueous soaps: Sodium octanoate and sodium dodecanoate (sodium laurate). *Colloids Surf., A* **1996**, *108* (2−3), 225−242.
(57) Varade, D.; Carriere, D.; Arriaga, L.; Fameau, A.-L.; Rio, E.; Langevin, D.; Drenckhan, W. On the origin of the stability of foams made from catanionic surfactant mixtures. *Soft Matter* **2011**, *7* (14), 6557−6570.
(58) Briceño-Ahumada, Z.; Langevin, D. On the influence of surfactant on the coarsening of aqueous foams. *Adv. Colloid Interface Sci.* **2017**, *244*, 124−131.
(59) Georgieva, D.; Cagna, A.; Langevin, D. Link between surface elasticity and foam stability. *Soft Matter* **2009**, *5* (10), 2063−2071.
(60) Carrier, V.; Colin, A. Coalescence in draining foams. *Langmuir* **2003**, *19* (11), 4535−4538.
(61) Kristen-Hochrein, N.; Schelero, N.; Von Klitzing, R. Effects of oppositely charged surfactants on the stability of foam films. *Colloids Surf., A* **2011**, *382* (1), 165−173.
(62) Blute, I.; Jansson, M.; Oh, S.; Shah, D. The molecular mechanism for destabilization of foams by organic ions. *J. Am. Oil Chem. Soc.* **1994**, *71* (1), 41−46.
(63) Arnould, A.; Cousin, F.; Chabas, L.; Fameau, A.-L. Impact of the molar ratio and the nature of the counter-ion on the self-assembly of myristic acid. *J. Colloid Interface Sci.* **2018**, *510*, 133.
(64) Fameau, A.-L.; Arnould, A.; Lehmann, M.; von Klitzing, R. Photoresponsive self-assemblies based on fatty acids. *Chem. Commun.* **2015**, *51* (14), 2907−2910.
(65) Chiappisi, L. Polyoxyethylene alkyl ether carboxylic acids: an overview of a neglected class of surfactants with multiresponsive properties. *Adv. Colloid Interface Sci.* **2017**, *250*, 79.

DOI: 10.1021/acs.langmuir.8b02261
Langmuir 2018, 34, 11076−11085